UDC519.6:537.871.3:621.746.01

Present Status of Electromagnetic Field Analysis and Its Application to Flow Control in Continuous Caster Molds

Kenji Umetsu*1
Keisuke Fujisaki*1
Kiyoshi Wajima*1
Shunji Nishi*2
Kenzo Sawada*1
Takatsugu Ueyama*1

Abstract:

The software FLEDY, which uses the finite element method (FEM) for the three-dimensional analysis of electromagnetic fields, has been applied to the design and development of electromagnetic energy utilizing equipment in ironmaking and steelmaking processes. The basic equations of the electromagnetic field analysis software FLEDY, its functions, and its fast computing methods are described. The application of FLEDY to assist in the control of molten steel flow within a continuous caster mold is discussed as an example of its usage in the steel industry.

1. Introduction

Two of the authors already explained the three-dimensional, general-purpose, FEM electromagnetic field analytical software FLEDY in a previous issue of the Nippon Steel Technical Report (NSTR)[1]. Originally developed as an aid to develop electromagnetic energy utilizing equipment in ironmaking and steelmaking, FLEDY has been used in the design and development of equipment, and has been functionally improved for that purpose. Nippon Steel's Electronics & Information Systems Division started marketing it in 1989, and has since supplied it to many users in and outside the Company.

This paper touches on the basic equations for analyzing electromagnetic fields, the functions of FLEDY, and the techniques employed to increase the speed of computation. The improvement of FLEDY's computing speed has been particularly striking. New techniques such as the ICCG (incomplete Cholesky conjugate gradient) method and the edge element method are discussed in detail. The increased speed of solving simultaneous linear equations by parallel processing is described in depth as well. The use of FLEDY in controlling the flow of molten steel in a continuous caster mold is introduced as an example of a steelmaking application. A practical technique for electromagnetic field analysis is used in this example.

*1 Technical Development Bureau
*2 Electronics & Information Systems Division

2. Basic Equations for Electromagnetic Field Analysis[1,2]

FLEDY consists of two programs: one program for solving magnetostatic field and eddy current field problems and another for addressing electrostatic and temperature fields. The basic parts of the two programs are described here.

2.1 Basic equations for eddy current field

The basic equations for an electromagnetic field are the following four Maxwell's equations:

$$\nabla \times \mathbf{H} = \mathbf{J} + \frac{\partial \mathbf{D}}{\partial t} \quad \cdots\cdots(1)$$

$$\nabla \times \mathbf{E} = -\frac{\partial \mathbf{B}}{\partial t} \quad \cdots\cdots(2)$$

$$\nabla \cdot \mathbf{B} = 0 \quad \cdots\cdots(3)$$

$$\nabla \cdot \mathbf{D} = \rho \quad \cdots\cdots(4)$$

where **E** is electric field intensity; **B** is magnetic flux density; **D** is electric flux density; **H** is magnetic field intensity; ρ is electric charge density; and **J** is electric current density. The following relations, called constitutive equations, exist between the vectors in the above equations:

$$\mathbf{B}=\mu\mathbf{H},\quad \mathbf{D}=\varepsilon\mathbf{E} \qquad \cdots\cdots(5)$$

where μ and ε refer to permeability and permittivity, respectively, and are generally tensor quantities. Usually in these equations, the vectors are replaced by quantities called the vector potential **A** and scalar potential ϕ, respectively.

$$\mathbf{B}=\nabla\times\mathbf{A},\quad \mathbf{E}=-\frac{\partial\mathbf{B}}{\partial t}-\nabla\phi \qquad \cdots\cdots(6)$$

This is the most standard transformation method capable of deriving physical quantities about a given electromagnetic field.It is highly versatile, and is called the **A**-ϕ method. Since the presence of the vector potential **A** is already confirmed[3], the **A**-ϕ method is adopted in most of today's electromagnetic field analytical programs.

The following equations obtained by ignoring the right-hand-side second term or displacement current term of Eq. (1) and using Eqs. (5) and (6) as well as the Joule's law are used as the basic equations for the eddy current field:

$$\nabla\times(\mu^{-1}\cdot\nabla\times\mathbf{A})=\mathbf{J}_o+\mathbf{J}_e \qquad \cdots\cdots(7)$$

$$\nabla\cdot(\mathbf{J}_o+\mathbf{J}_e)=0 \qquad \cdots\cdots(8)$$

$$\mathbf{J}_e=\sigma\cdot\mathbf{E}=-\sigma\cdot\left(\frac{\partial\mathbf{A}}{\partial t}+\nabla\phi\right) \qquad \cdots\cdots(9)$$

where $\mathbf{J}_o$ is exciting current density and $\mathbf{J}_e$ is eddy current density. An electrostatic field problem can be solved by using Eq. (7) alone and putting $\mathbf{J}_e$ at 0. Eq. (9) contains a time differential term and must be discretized with respect to time as well. An eddy current field is quasi-stationary. That is, a sinusoidal AC problem can be solved by the $j\omega$ method whereby the differential operator is replaced by the complex number $j\omega$, where j is the imaginary unit and ω is angular frequency (the time variation corresponds to the phase variation). For a transient problem, Eq. (9) is discretized by the backward finite difference method formulated as follows:

$$\frac{\partial\mathbf{A}_{i+1}}{\partial t}=\frac{\mathbf{A}_{i+1}-\mathbf{A}_i}{\Delta t} \qquad \text{(where } \Delta t \text{ is time increment)}$$

The Galerkin method is applied to the basic equations thus obtained, and the basic equations are then discretized by the finite element method. The developed simultaneous linear equations are summarized into the following equations, where the square brackets [ ] and the braces { } denote a matrix and a vector, respectively:

$$[\mathbf{K}(\mu,\sigma,\omega)]\{\mathbf{A}\}=\{\mathbf{F}(\mathbf{J}_o)\} \qquad \text{(Quasi-stationary)}$$

$$[\mathbf{K}(\mu,\sigma)]\{\mathbf{A}_{t+\Delta t}\}=[\mathbf{M}(\Delta t,\sigma)]\{\mathbf{A}_t\}+\{\mathbf{F}_{t+\Delta t}(\mathbf{J}_o)\} \qquad \text{(Transient)}$$

The discretization procedure and equations are described in detail in Reference2). The same discretization procedure also applies to the next electric field analysis, except for the basic equation.

2.2 Basic equation for electric field

Poisson's or Laplace's differential equation is a basic equation for understanding electrostatic fields and steady-state electric current fields. The FLEDY program uses the following diffusion equation as the basic equation and can calculate the temperature field as well as the electrostatic field and the steady-state electric current field.

$$\nabla\cdot(\varkappa\cdot\nabla\phi)+Q=C\frac{\partial\phi}{\partial t} \qquad \cdots\cdots(10)$$

where ϕ is potential or temperature; $\varkappa$ is permittivity, electric conductivity or thermal conductivity; C is electrostatic capacity or heat capacity; and Q is electric charge density, current source density or heat source density. The Crank-Nicolson method is adopted for the development of the time derivative[4]. The Galerkin method is applied to Eq. (10), and the simultaneous linear equations developed by the finite element method are represented by the following equation:

$$[K(\varkappa)]\{\phi\}+[C]\frac{\partial}{\partial t}\{\phi\}=\{Q\}$$

then, the Crank-Nicolson expansion becomes:

$$\left(\frac{[C]}{\Delta t}+\frac{1+\beta}{2}[K]\right)\{\phi\}_{t+\Delta t}=\left(\frac{[C]}{\Delta t}+\frac{1-\beta}{2}[K]\right)\{\phi\}_t-\frac{1}{2}\{(1+\beta)\{Q\}_{t+\Delta t}+(1-\beta)\{Q\}_t\}$$

where β is a parameter that assumes the value of $-1\leq\beta\leq1$.

3. Analytical Functions of FLEDY

The above-mentioned basic equations can be used to analyze various electromagnetic fields. There are several functions that are necessary or effective for solving concrete problems. Such analytical functions of FLEDY are described below. Besides those described here, there are many additional analytical functions such as for computing the Maxwell stress, velocity term, permanent magnet, material anisotropy, and magnetic energy.

3.1 Nonlinear analytical functions

As the magnetic field intensity increases, actual magnetic materials generally decline in magnetic permeability or undergo what is called magnetic saturation. Solutions cannot be obtained without using nonlinear analysis. Although there are several nonlinear analytical techniques, FLEDY has the simple iterative method of iteratively correcting the permeability μ in Eq. (7) and the Newton-Raphson method[5] estimates the amount by which the potential is to be corrected on the basis of the Maxwell equations. The two methods can make the necessary corrections by referring to magnetization characteristic curves and can also refer to either the magnetic permeability, magnetic flux density or vector potential when judging convergence. The Newton-Raphson method tracks down the magnetic flux density by utilizing the tangent to the magnetization curve and is widely used in structural analysis, for example. Since its convergence is not high in electromagnetic field analysis, the relaxation coefficient was introduced on a trial basis[6], but not much improvement was obtained[7].

The previous report[1] touched on a new quasi-stationary nonlinear analytical technique termed the equivalent sinusoid method.

The equivalent sinusoid method later proved insufficient for problems containing the revolving of the magnetic field intensity **H** and the magnetic flux density **B**, so it was expanded to embrace revolving magnetic fields as well[8]. The expanded version also assumes the directional coincidence and anisotropy of **H** and **B**. The expansion causes little or no increase in computing time and provides approximately 20 times higher computing speed.

3.2 Voltage source analytical functions (circuit equations)[9]

Basic equations (7) and (8) assume that the exciting current density $\mathbf{J}_o$ is known. The voltage value of actual electric equipment is mostly referred to when operating or inspecting it, however. It is necessary to constitute basic equations that use the voltage value in place of the current value.

It is assumed that single-phase alternating current flows in the series circuit shown in **Fig. 1**. The circuit line current is put at $\mathbf{I}_o$ by ignoring the skin effect of the conductor. Assuming that the line current I_o flows in a coil with the cross-sectional area S_c and number of turns n_c, the following equation can be formed:

$$n_c I_o = S_c |\mathbf{J}_o| \qquad \cdots\cdots(11)$$

The series circuit is expressed by

$$(Z_o + R) I_o + j\omega\psi = V_o \qquad \cdots\cdots(12)$$

where ψ is the magnetic flux that interlinks with the coil and is expressed by the following equation with the use of the vector potential:

$$\psi = \frac{n_c}{S_c} \iint \left(\int \mathbf{A} \cdot d\mathbf{l}\right) dS \qquad \cdots\cdots(13)$$

Surface integration is performed with respect to the cross-sectional area of the coil, and line integration is performed along the length of the coil. The finite element region and circuit can be handled as a combined system by transforming Eqs. (7) and (12) with Eqs. (11) and (13) and solving them simultaneously with Eq. (8).

3.3 Leaf elements[10]

If a problem involves an extremely thin material with respect to its dimensions in the analytical domain, as is the case with magnetic head gaps or thin magnetic shields for MRI (magnetic resonance imaging), the scale difference adds a degree of numerical singularity into the simultaneous linear equations, producing a nonphysical solution. Enormous computing time will be required if the analytical domain is divided into a finer mesh to obtain the correct solution.

The leaf element method constitutes simultaneous equations by not making variables on adjacent nodes as the unknown variables but by making the difference between the variables as the unknown variable (called the relative potential). This achieved the desired accuracy and shortened computing time.

When the nodes i+1 and i are close to each other, the electromagnetic quantity A is transformed as follows:

$$A_{i+1} = A_i + \Delta_i$$

where Δ_i is the relative potential. The numerical singularity noted above can be completely eliminated by using Δ_i as the unknown variable in place of A_{i+1} and reconstituting the simultaneous equations.

An application example of the leaf element method is given here. A 1/8-scale model of a simple magnetic shield is illustrated in **Fig. 2**. The experiment was conducted to verify the validity of the leaf element method. Contour maps of the x-direction component of the magnetic flux density are prepared from the analytical and experimental results and are given in **Fig. 3**. Of the six contour maps, the three on the left side present the experimental results, and the three on the right side present the analytical results. **Fig. 3(a)** shows the contour maps without the magnetic

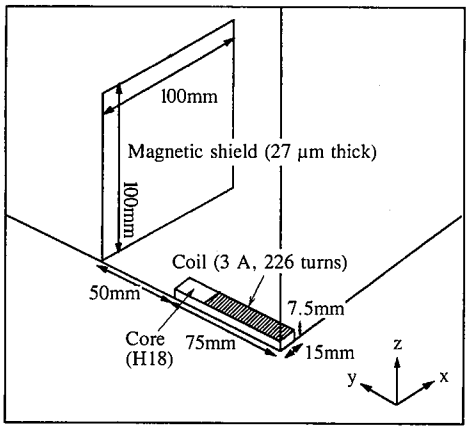

Fig. 2 1/8-scale model of magnetic shield (magnetostatic field)

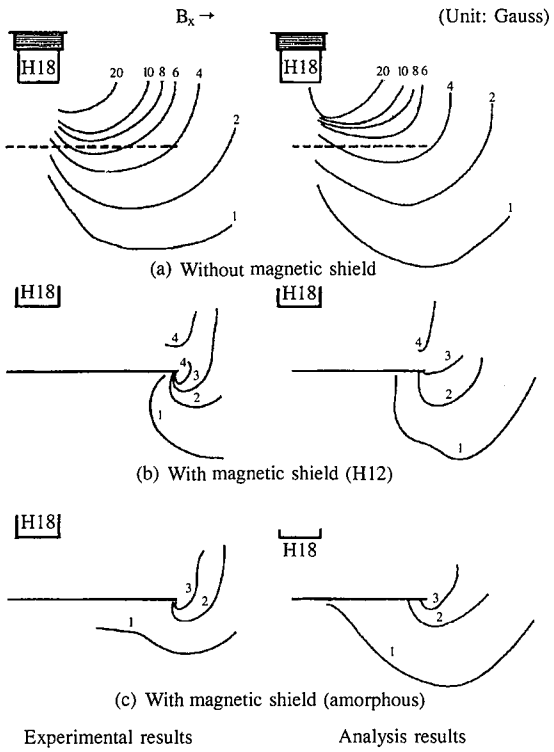

Fig. 3 Comparison of experimental and analysis results

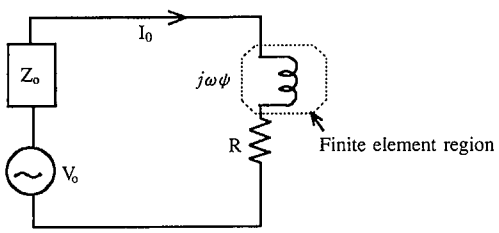

Fig. 1 Series circuit connected to voltage source

shield. From the two contour maps, it is evident that the volume ratio produces no effect in the leaf element method. From the contour maps of **Figs. 3(b)** and **3(c)**, it is evident that a valid solution is obtained in the presence of the magnetic shield. The accuracy of the solution is especially high with an amorphous shield of high permeability. When the magnetic shield was electrical steel H12 and the contour maps were computed by the conventional finite element method, the maximum magnetic flux expanded four times or more, and abnormally large vectors appeared in the air.

3.4 Floating node method[11]

The floating node is a constitutive node of a finite element that does not overlap with any other node except at the outermost boundary. Consider two nodes i and j, and assume another node p on the straight line connecting the nodes i and j. The node p is defined as a floating node. The physical quantity A_p at the node p is approximated by the following liner interpolation equation:

$$A_p = \alpha A_i + (1-\alpha) A_j$$

where α and $1-\alpha$ are the distance ratios of the node p with respect to the nodes i and j, respectively. The floating node is relative. The nodes i and j can be conversely interpolated from the node p and another node.

The floating node method has the following two advantages:

(1) Since the analytical domain can be divided finely in some portions and coarsely in other portions, the number of elements is reduced(**Fig. 4**[11]).

(2) Since inconsistent elements can be joined, mesh preparation and relative object movement can be easily handled.

An example of analysis made by using the advantage (2) is shown in **Figs. 5** and **6**. A model of a rotor with a periodic arrangement of electric current is shown in **Fig. 5**. The analytical result of the model by the floating node method is given in **Fig. 6** with vector potential contour lines. Despite the presence of many inconsistent nodes where the two regions meet, the contour lines are smoothly connected.

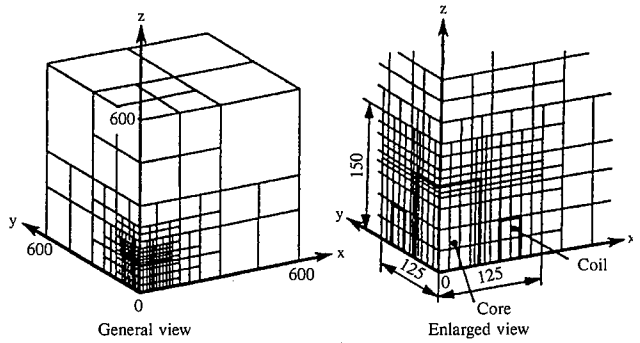

Fig. 4 Mesh plot containing floating nodes

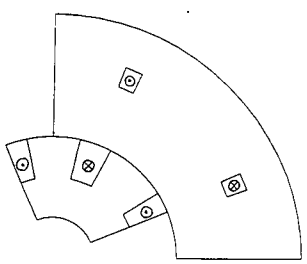

Fig. 5 Schematic of 1/4 model of rotor

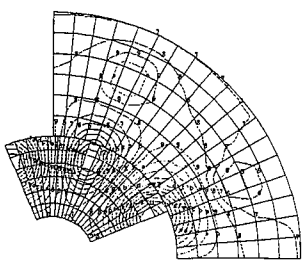

Fig. 6 Potential contour map

3.5 Coupled analytical functions[1]

Actual electromagnetic equipment involves not only electromagnetic phenomena, but also thermal phenomena and dynamic motions. When analysis with a high degree of reality is required or when the final quantity desired is not an electromagnetic one, it is necessary to analyze electromagnetic phenomena coupled with other phenomena. FLEDY can handle problems where electromagnetic phenomena are coupled with thermal and fluid flow phenomena. This capability is one of its main features.

3.5.1 Coupled analysis with temperature field

The problems of conductive heating and inductive heating must be solved as coupled with temperature fields. FLEDY allows such problems to be analyzed with a high degree of reality through data exchange. The following procedure is employed:

(1) With the $j\omega$ method, obtain the amount of heat generated by induced current.

(2) Compute the temperature over some time steps from the amount of heat generation.

(3) Update the physical quantity (magnetic permeability or electric conductivity) from the temperature.

These three steps are repeated until the end of the analysis.

For DC conductive heating, obtaining the amount of heat generated in step(1) by the electric field analytical program is sufficient. Since the change with time in the electromagnetic field is usually greater than that with temperature, electromagnetic field analysis is sufficiently in the quasi-stationary state and is performed with a shorter computing time. Since the variations in the electromagnetic properties of the material can be considered with the temperature change, the phenomena involved can be accurately reproduced. Both programs can use the same mesh.

3.5.2 Coupled analysis with fluid flow field

Electromagnetic fluid problems such as those involved with electromagnetic stirring must be coupled with fluid flow. FLEDY can compute the Lorentz forces acting on conductors. The behavior of fluids under electromagnetic forces can be thus reproduced to some degree by the following procedure:

(1) The Lorentz force is time averaged by the $j\omega$ method in FLEDY.

(2) The time-averaged Lorentz force is transferred to another fluid analysis program and substituted into the volume force term of the Navier-Stokes equation to compute the fluid velocity.

Mutual computation is not performed as done for the analysis of the electromagnetic field coupled with the fluid field. This method produces a satisfactory solution when the time scale of the fluid field is far greater than that of the electromagnetic field. Since the electromagnetic force and the fluid velocity do not generally agree in the distribution region, however, the mesh must be prepared by paying attention to this difference. An actual example of analysis performed by this method is described in detail in chapter 5.

4. High-Speed Computing Techniques

Computing capability depends on computer capacity and speed. It is desirable that a solution be obtained with a small computing capacity and a short computing procedure. This objec-

tive may be accomplished by increasing the speed of either the algorithm or computer. The iterative solution method is typical of the former method, and parallel processing is representative of the latter. The two methods are discussed in detail here.

4.1 ICCG method[12]

Simultaneous linear equations may be solved by direct or iterative methods. FLEDY has both methods. The direct method is the modified Cholesky method, and the iterative method is the incomplete Cholesky conjugate gradient (ICCG) method. Problems composed of large simultaneous linear equations and high in convergence can be solved by the ICCG method in a far shorter computing time than possible with the modified Cholesky method. Computational examples are given in **Table 1**. The ICCG method increases the computing speed by seven times. Refer to section 4.3 for the algorithm for the ICCG method.

The ICCG method is superior in not only speed but also convergence. If the problem does not converge after many iterations by the ICCG method, it is often ill-natured or ill-conditioned. In other words, whether or not specific problems are ill-conditioned can be known to some degree from the level of convergence obtained by the ICCG method.

4.2 Edge element method[13]

Since electromagnetic field analysis techniques have advanced on the basis of structure analysis techniques, they are fundamentally the same as structure analysis techniques. A new element method, suited for handling electromagnetic fields, which is basically composed of vector quantities and called the edge element method, was developed in the late 1980s and has been studied by many researchers since.

The edge element method is characterized by the assignment of variables. The nodal element method assigns all necessary physical quantities to each node and constitutes a vector quantity from three variables at each node. On the other hand, the vector quantity is represented by the vector composition of edge elements. A variable is assigned to each edge, and the direction of the vector is expressed by the direction of the edge (see **Fig. 7**). There are three reasons why the edge element method is spotlighted. Unlike the conventional element methods, the edge element method can directly represent vector quantities by vector interpolation functions. Accuracy is very high for electromagnetic wave problems, as compared with the nodal element method, and higher computing speed can be achieved. With the edge element method alone, however, increased computing speed cannot be always accomplished.

As far as the computing speed increase is concerned, the edge element method and the nodal element method, both being direct methods, are approximately the same in the spread of the matrix band width and have no factors conductive to higher speed. When an iterative method such as the ICCG method is used, nonzero components in the matrix suffice, and their number is

Table 1 Effects of ICCG method and edge element method on computing time

	Node element method + modified Cholesky method	Node element method + ICCG method	Edge element method + ICCG method
Number of iterations	—	438	220
Computing time	859 min	123 min	40 min

The holed model of the Institute of Electrical Engineers of Japan (number of elements:5,445; total number of nodes: 6,368)
ICCG convergence criterion: 5.0×10^{-5}; computer: Sun Microsystems SPARC Station 2

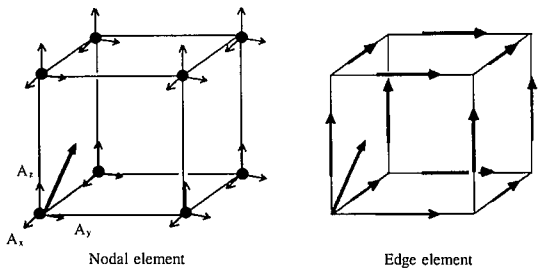

Fig. 7 Nodal element and edge element

usually about a half to one-third of that of nodal elements. In addition, the required number of iterations is a few times smaller than for the nodal element method, resulting in higher speed. An example of the edge element method used as incorporated into FLEDY to achieve higher speed is given in **Table 1**. The combination of the edge element method with the ICCG method is at least three times faster than the combination of the nodal element method with the ICCG method and is more than 21 times faster than the standard combination of the nodal element method and the modified Cholesky method.

4.3 Speed increase by parallel processing[14]

The FLEDY parallel processing technique solves simultaneous linear equations by assigning them to multiple processors. The hardware is composed of Transputers or Inmos-developed processors with local memories, and a distributed-memory MIMD (multiple-instruction multiple-data) architecture. The MIMD architecture has no limitations on the number of processors to be used and is expected to become a mainstream parallel processing architecture in the future.

Parallelization was implemented for both the modified Cholesky method and the ICCG method. Parallelzation for the ICCG method, which is increasing in usage is described here. The algorithm of the ICCG method for the simultaneous linear equations $Ax = b$ is as given below.

(Incomplete Cholesky decomposition and initial value setup)

$$K=(U^TDU)^{-1},\ x_0=Kb,\ r_0=b-Ax_0,\ p_0=Kr_0$$

(Iterative computation: kth iteration)

While $\| r_k \| > \varepsilon \| b \|$

$$\alpha_k = (r_k,Kr_k)/(p_k,Ap_k)$$
$$x_{k+1} = x_k+\alpha_k p_k$$
$$r_{k+1} = r_k-\alpha_k Ap_k$$
$$\beta_k = (r_{k+1},Kr_{k+1})/(r_k,Kr_k)$$
$$p_{k+1} = Kr_{k+1}+\beta_k p_k$$
$$k = k+1$$

where U^T, D, and U are the lower triangular, diagonal, and upper triangular matrixes obtained when the overall coefficient matrix A is subjected to the incomplete Cholesky decomposition, respectively, and ε is the convergence criterion.

Parallelization is difficult to perform with the incomplete Cholesky decomposition and with the backward substitution after each iteration. The degree of parallelization for these operations governs the computing speed. To facilitate this parallelization, incomplete Cholesky decomposition is performed only on the nonzero components in each block in the band matrix shown in

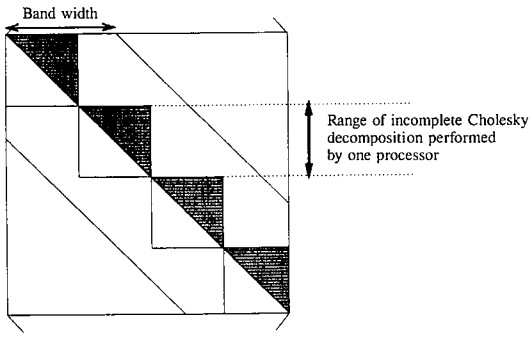

Fig. 8 Parallelization of incomplete Cholesky decomposition

Table 2 Computing time(ICCG method, diagonal terms multiplied by 1.2, unit: s)

Number of processors	Processing time	Data transfer	Preprocessing	Number of iterations
1	1858	21	134	92
2	1291	22	54	146
4	805	22	20	202
8	481	22	8	247
16	284	26	3	265

Number of matrix dimensions: 2,224, band width: 392, number of nonzero components: 78,528, CPU: Transputers (Inmos)

Fig. 8. The size of one side of the block is equal to the number of rows covered by one processor. Data communication between the blocks is eliminated in the incomplete Cholesky decomposition and is reduced in the backward substitution after each iteration. Increasing the number of processors decreases the range of incomplete Cholesky decomposition and increases the number of iterations. At present, there are no iterative methods that can achieve high parallelization and high convergence at the same time. **Table 2** shows the computing time by the parallel processing technique. The reduction in total computing time is prevented by the increase in the number of iterations. The modified Cholesky method is highly effective as far as parallel processing is concerned. When selecting a solution method it is necessary to consider such factors as model size, computer capacity, and total computing time.

5. Application to Fluid Flow Control in Mold[15,16]

5.1 In-mold fluid flow control and electromagnetic stirrer

The ability to control the quality of steel in a steelmaking process is decisively important from a production point of view. Continuous casting is a principal determinant of steel quality. Once the molten steel that has been refined in the basic oxygen furnace (BOF) is solidified on the continuous caster, the surface properties of the cast steel cannot be greatly changed, neither can nonmetallic inclusions be removed from the cast steel in subsequent steps. To improve the surface quality of steel and remove nonmetallic inclusions, the molten steel in the solidification region is induced to move by an in-mold electromagnetic stirrer.

The electromagnetic stirrer causes the molten steel to flow as a result of the electromagnetic force produced by an electromagnetic coil. It is necessary to first grasp the electromagnetic phenomena at work by electromagnetic field analysis and then clarify the flow characteristics of the molten steel by fluid flow analysis. Since the object to be stirred is a fluid, the magnitude of the electromagnetic force is as important as its distribution. Usually, the electromagnetic stirrer is equivalent to the primary coil of a linear induction motor, and the molten steel is equivalent to the secondary side of the linear induction motor. The moving magnetic field produced by the coil interlinks with the molten steel and induces an electric current in the molten steel. The moving magnetic field and the induced current produce the Lorentz force, which in turn stirs the molten steel.

An example of an in-mold electromagnetic stirrer is illustrated in **Fig. 9**. The mold is made of copper plates of high enough thermal conductivity for efficient heat extraction and fast solidification of the molten steel. Each copper plate is reinforced with an outer stainless steel plate. The coil is installed outside of the copper and stainless steel plates. Since the distance between the coil and molten steel is large, the pole pitch must be also large. When the pole pitch is large, magnetic field leakage increases. To suppress magnetic field leakage and accomplish space savings around the mold, the coils is tightly wound around the core. The coils are installed parallel in the broad sides of the mold.

5.2 Magneto-fluid analysis technique

The values for Lorentz force obtained by FLEDY were transferred as external force values to the fluid flow analysis software developed at Nippon Steel and were used as data for computing the molten steel velocity. Here, it was assumed that the synchronous velocity of the magnetic field produced by the linear motor was much higher than the flow velocity of the molten steel and that the fluid field had no effect on the electromagnetic field.

The electromagnetic field analysis modeled the meniscus area where the electromagnetic field is concentrated, and the fluid field analysis modeled the long mold filled with the molten steel. Spatially, a three-phase alternating current is periodically applied to the coils to form the moving magnetic field (the moving direction is counterclockwise when seen from above).

The linear structure of the coils can produce unbalanced three-phase components in the electric current. Since the operating frequency is a few hertz at most, however, the primary DC resistance components predominate over the inductance components on which the unbalance exerts an effect. A source of current balanced in the three phases was used for the analysis. The cores were free from magnetic saturation and constant in relative permeability.

The Lorentz force distribution near the meniscus as obtained by the electromagnetic field analysis and seen from above is

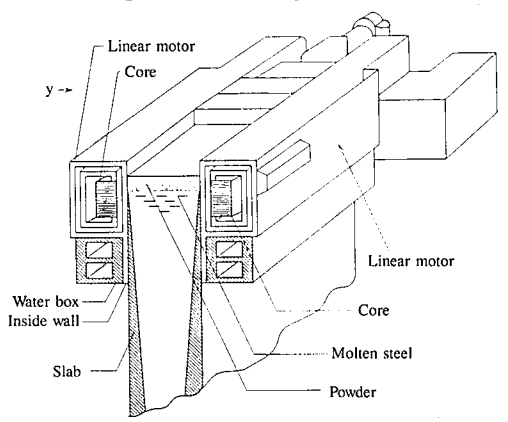

Fig. 9 Schematic illustration of in-mold electromagnetic stirrer

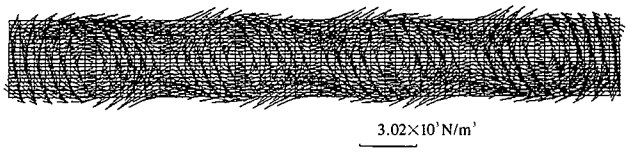

Fig. 10 Top view of Lorentz force distribution near meniscus

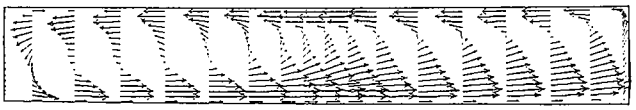

Fig. 11 Top view of velocity distribution near meniscus

shown in **Fig. 10**. The velocity distribution derived from the Lorentz force distribution is shown in **Fig. 11**. Rotary stirring always produces nodes in the Lorentz force distribution. The effect of the nodes on the velocity distribution was found to be small.

6. Conclusions

The present analytical functions and application examples of the three-dimensional general-purpose electromagnetic field analysis software FLEDY have been described. The functions have been added through the use of FLEDY as an aid in the development of specific electrical equipment and electromagnetic energy utilizing equipment used in ironmaking and steelmaking processes. The usefulness of FLEDY has been indicated through its application to the electromagnetic stirring of molten steel in the mold of a continuous caster. As can be seen from this example, the synergistic effect of computer environment advancement and algorithm improvement has increased the reality of numeric approaches to actual problems. Under these circumstances, numeric analysis techniques are expected to find increasing use in applications to actual processes.

Acknowledgments

The authors would like to thank Takuma Nakatsukasa and Shinji Sonoda of Yawata Computer Center Co., Ltd., Tetsuya Shimizu of Nittetsu Elex Co., Ltd., Yasuhiro Mizutani of Nippon Steel Information & Communication Systems Inc., and Takashi Mori of Kyoei Electronics Co., Ltd., for their cooperation in the development and application of FLEDY.

References

1) Ueyama, T., Umetsu, K.: Development of Three-Dimentional Electromagnetic Field Analysis Code FLEDY. Shinnittetsu Giho. (341), 23 (1991)
2) Ueyama, T., Shinkura, K., Ueda, R.: Fundamental Equations for Eddy Current Analysis by Using the A-ϕ Method and 3-D Analysis of a Conducting Fluid. IEEE Trans. on Magnetics. MAG-25 (5), 4153-4155 (1989)
3) Tonomura, A.: Applications of electron holography. Reviews of Modern Physics. 59, 639 (1987)
4) Japan Society of Mechanical Engineers: Computer Analysis of Heat and Flow. Corona Publishing Co., Ltd., 1986, p.178
5) Nakata, T., Takahashi, N.: Finite Element Methods for Electrical Engineering, Second Edition. Morikita Shuppan, 1982, p.200
6) Fujiwara, K., Nakata, T., Okamoto, N., Muramatsu, K.: Method for Determining Relaxation Factor for Modified Newton-Raphson Method. IEEE Trans. on Magnetics. MAG-29 (2), 1962-1965 (1993)
7) Fujiwara, K., Nakata, T., Ogino, T., Kondoh, S.: Investigation on Simple Iterative Method for Nonlinear Magnetic Field Analysis. 1995 National Convention of the Institute of Electrical Engineers of Japan, No. 896
8) Sadaki, J., Umetsu, K., Wajima, K., Ueyama, T.: Expansion of Equivalent Sinusoidal Method. Papers of Technical Meeting on Static Apparatus and Rotating Machinery, IEE Japan, SA-94-10, RM-94-74, 1991
9) Ueyama, T., Nishi, S., Wajima, K., Umetsu, K., Nishisaka, T.: 3-D Analysis of Electromagnetic Field Including Conductors Connected with Voltage Sources. IEEE Trans. on Magnetics. MAG-29 (2), 1385-1388 (1993)
10) Ueyama, T., Umetsu, K., Hirano, Y.: Magnetic Shielding Analysis by FEM Using Relative Potential. IEEE Trans. on Magnetics. MAG-26 (5), 2202 (1990)
11) Muramatsu, K., Nakata, T., Takahashi, N., Fujiwara, K.: 3-D Adaptive Mesh Refinement Using Nonconforming Elements. IEEE Trans. on Magnetics. MAG-29 (2), 1479-1482 (1993)
12) Murata, K., Natori, T., Karaki, Y.: Large-Scale Numerical Simulation. Iwanami Shoten, 1990, p.102
13) Fujiwara, K.: 3-D Computation Using Edge Elements. Proceedings of 5th IGTE Symposium on Numerical Field Calculation in Electrical Engineering, 1992, p.185-221
14) Ueyama, T., Kaneko, H., Umetsu, K.: Parallel Processing. 3rd Seminar on Electromagnetic Field Analysis, 1992
15) Fujisaki, K., Sawada, K., Ueyama, T., Okazawa, K., Toh, T., Takeuchi, E.: Fundamental Electromagnetic Characteristics of In-mold Electromagnetic Stirring Continuous Casting. Papers on International Symposium on Electromagnetic Processing of Materials, ISIJ, Nagoya, 1994, p.272
16) Okazawa, K., Toh, T., Takeuchi, E., Fujisaki, K.: Characteristics of Fluid Flow Driven by Linear Motor. Papers on International Symposium on Electromagnetic Processing of Materials, ISIJ, Nagoya, 1994, p.278